http://hdl.handle.net/2440/99216

Finite Nuclei in the Quark-Meson Coupling Model

J. R. Stone,[1,2] P. A. M. Guichon,[3] P. G. Reinhard,[4] and A. W. Thomas[5]

[1]*Department of Physics, University of Oxford, Oxford OX1 3PU, United Kingdom*
[2]*Department of Physics and Astronomy, University of Tennessee, Knoxville, Tennessee 37996, USA*
[3]*SPhN-IRFU, CEA Saclay, F91191 Gif sur Yvette, France*
[4]*Institut für Theoretische Physik II, Universität Erlangen, D-91058 Erlangen, Germany*
[5]*ARC Centre of Excellence in Particle Physics at the Terascale and CSSM, Department of Physics,
University of Adelaide, SA 5005 Australia*

We report the first use of the effective quark-meson coupling (QMC) energy density functional (EDF), derived from a quark model of hadron structure, to study a broad range of ground state properties of even-even nuclei across the periodic table in the nonrelativistic Hartree-Fock + BCS framework. The novelty of the QMC model is that the nuclear medium effects are treated through modification of the internal structure of the nucleon. The density dependence is *microscopically* derived and the spin-orbit term arises naturally. The QMC EDF depends on a single set of four adjustable parameters having a clear physics basis. When applied to diverse ground state data the QMC EDF already produces, in its present simple form, overall agreement with experiment of a quality comparable to a representative Skyrme EDF. There exist, however, multiple Skyrme parameter sets, frequently tailored to describe selected nuclear phenomena. The QMC EDF set of fewer parameters, derived in this work, is not open to such variation, chosen set being applied, without adjustment, to both the properties of finite nuclei and nuclear matter.

Since the pioneering work of Vautherin and Brink [1], effective nuclear forces of the Skyrme type have proved to be a powerful phenomenological tool in the study of many aspects of nuclear structure (for reviews, see [2–4]). The Skyrme energy density functional (EDF) for self-consistent mean-field models of the Hartree-Fock (HF) type is derived from the Skyrme force using low-momentum expansion. The functional contains all conceivable bilinear couplings of densities and currents up to second order in derivatives. This approach introduces 23 coupling constants (parameters) which are, in principle, density dependent. Taking a minimalistic approach [4] the number of the constants can be reduced to ∼10, which have to be fitted to empirical data, usually nuclear ground state properties. Because of correlations in experimental data, variable sensitivity of individual parameters to data and correlations between the parameters themselves, no single optimal parameter set has yet been identified. Presently, many sets of the Skyrme EDF parameters exist, making it difficult to interpret and reliably predict nuclear properties.

Given the power of the mean-field approach with the Skyrme EDF, we adopted this approach with a quark-meson coupling (QMC) EDF. In the QMC model, developed by Guichon and collaborators [5,6], the nuclear system is represented as a collection of confined clusters of valence quarks. Using the MIT bag model [7], it can be shown that when the quarks in one nucleon interact *self-consistently* with the quarks in the surrounding nucleons by exchanging a σ meson (a simple representation of the Lorentz scalar-isoscalar interaction known to dominate the intermediate range attraction between nucleons), the effective mass of a nucleon in medium is no longer linear in the scalar mean field (σ) and is expressed as $M_N^* = M_N - g_{\sigma N}\sigma + (d/2)(g_{\sigma N}\sigma)^2$. By analogy with electromagnetic polarizabilities, the coefficient d, calculated in terms of the nucleon internal structure, is known as the "scalar polarizability" [5]. The appearance of this term in the nucleon effective mass is sufficient to lead to nuclear saturation.

To clarify differences between the Skyrme and QMC EDF's, we write the QMC EDF adopted in this work $\langle H(\vec{r})\rangle = \rho M_N + (\tau/2M_N) + \mathcal{H}_0 + \mathcal{H}_3 + \mathcal{H}_{\mathrm{eff}} + \mathcal{H}_{\mathrm{fin}} + \mathcal{H}_{\mathrm{so}}$ using notation and definitions from [8,9], where

$$\mathcal{H}_0 + \mathcal{H}_3 = \left(-\frac{3G_\rho}{32} + \frac{3G_\omega}{8} - \frac{G_\sigma}{2(d\rho G_\sigma + 1)} + \frac{G_\sigma}{8(d\rho G_\sigma + 1)^3}\right)\rho^2 + \left(\frac{5G_\rho}{32} - \frac{G_\omega}{8} + \frac{G_\sigma}{8(d\rho G_\sigma + 1)^3}\right)(\rho_n - \rho_p)^2,$$

$$\mathcal{H}_{\mathrm{eff}} = \left[\left(\frac{G_\rho}{8m_\rho^2} - \frac{G_\sigma}{2m_\sigma^2} + \frac{G_\omega}{2m_\omega^2} + \frac{G_\sigma}{4M_N^2}\right)\rho_n + \left(\frac{G_\rho}{4m_\rho^2} + \frac{G_\sigma}{2M_N^2}\right)\rho_p\right]\tau_n + p \leftrightarrow n,$$

$$\mathcal{H}_{\mathrm{fin}} = \left[\left(\frac{3G_\rho}{32m_\rho^2} - \frac{3G_\sigma}{8m_\sigma^2} + \frac{3G_\omega}{8m_\omega^2} - \frac{G_\sigma}{8M_N^2} \right) \rho_n + \left(-\frac{3G_\rho}{16m_\rho^2} - \frac{G_\sigma}{2m_\sigma^2} + \frac{G_\omega}{2m_\omega^2} - \frac{G_\sigma}{4M_N^2} \right) \rho_p \right] \nabla^2(\rho_n) + p \leftrightarrow n,$$

$$\mathcal{H}_{so} = \vec{\nabla} \cdot \vec{J}_n \left[\left(-\frac{3G_\sigma}{8M_N^2} - \frac{3G_\omega(2\mu_{\mathrm{is}} - 1)}{8M_N^2} - \frac{3G_\rho(2\mu_{\mathrm{iv}} - 1)}{32M_N^2} \right) \rho_n + \left(\frac{G_\omega(1 - 2\mu_{\mathrm{is}})}{4M_N^2} - \frac{G_\sigma}{4M_N^2} \right) \rho_p \right] + p \leftrightarrow n,$$

with $G_\sigma = g_{\sigma N}^2/m_\sigma^2$, $G_\omega = g_{\omega N}^2/m_\omega^2$, and $G_\rho = g_{\rho N}^2/m_\sigma^2$, where $g_{\sigma N}$, $g_{\omega N}$, and $g_{\rho N}$ are free nucleon-meson coupling constants [8]. There are two basic differences between this and the Skyrme EDF. The QMC expression contains, in addition to the standard point coupling terms ρ^2, $\rho\tau$, $\rho\Delta\rho$, the density dependent term involving inverse powers of $(1 + d\rho G_\sigma)$ and the spin-orbit term $\propto \rho\nabla J$. Both the more complicated density dependence and the spin-orbit term arise naturally from the model [10,11] and it does not require additional parameters.

This Letter presents a comparison of results obtained with QMC EDF, in its present simple form, with those of a representative Skyrme EDF. The first step is to determine the four adjustable parameters of the model, the couplings G_σ, G_ω, and G_ρ and the mass m_σ of the σ meson (constrained as 650 MeV $< m_\sigma <$ 750 MeV). This was done in two stages. First, the parameters were constrained by properties of symmetric infinite nuclear matter at saturation, including their uncertainty. We required -17 MeV $< E_0 < -15$ MeV, $0.14\,\mathrm{fm}^{-3} < \rho_0 < 0.18\,\mathrm{fm}^{-3}$ for the saturation energy and density and 28 MeV $< S_0 < 34$ MeV, $L > 20$ MeV, and 250 MeV $< K_0 <$ 350 MeV for the symmetry energy, its slope and the incompressibility. The remaining parameters of the model, the meson masses, and the isoscalar and isovector magnetic moments, which appear in the spin-orbit interaction [6,12,13], were taken at their physical values. The MIT bag radius R_B was set to 1 fm. This procedure yielded limits 10.2 fm$^2 < G_\sigma <$ 12.65 fm^2, 6.95 fm$^2 < G_\omega <$ 8.90 fm^2, and 6.20 fm$^2 < G_\rho <$ 8.80 fm^2.

Second, to narrow down the limits, the parameters were further constrained by specific ground state properties of selected nuclei. The QMC EDF has been incorporated into the HF + BCS code SKYAX [14], allowing for axially symmetric and reflection-asymmetric shapes. The data set consisted of selected binding energies, rms and diffraction charge radii, surface thickness of the charge distributions, the proton and neutron pairing gaps, and the spin-orbit splitting and energies of single-particle proton and neutron states, distributed across the nuclear chart. The best parameter set was sought using the fitting protocol developed by Klüpfel et al. [15]. In addition to the four parameters of the QMC EDF, two strengths (protons, neutrons) for volume pairing in the BCS framework [3] were included in the fit.

The overall best fit was given by a single set of QMC parameters: $G_\sigma = 11.85 \pm 0.02$ fm^2, $G_\omega = 8.27 \pm 0.02$ fm^2, $G_\rho = 7.68 \pm 0.03$ fm^2, and $m_\sigma = 722 \pm 1$ MeV. Note that the nonrelativistic form of the functional used here differs from the relativistic form used in [16] with the consequence the parameter values differ. The fitted parameters given above yield for nuclear matter properties $E_0 = -16.0 \pm 0.2$ MeV, $\rho_0 = 0.153 \pm 0.003$ fm^{-3}, $S_0 =$ 30 MeV (fixed), and $L = 23 \pm 4$ MeV within the desired range, but, however, the value $K_0 = 340 \pm 3$ MeV considerably higher than $K_0 \sim 220$–240 MeV, frequently adopted in nonrelativistic nuclear matter calculations. That value mainly originated from analysis of giant monopole resonance (GMR) data available in the 1980s, using a Skyrme interaction [17]. Typical relativistic mean field calculations agree with data better at K_0 around 270 MeV. Recently, Stone et al. [18] analyzed all GMR data available to date, in a way independent of the choice of nuclear interaction, showing that the limits on K_0 are $250 < K_0 < 315$ MeV. As an additional comment we note that the relativistic version [19] of the QMC EDF, previously applied to cold uniform matter, showed that the contribution of a long-range Yukawa single pion exchange lowered the incompressibility from 340 MeV to ~ 300 MeV, compatible with results in [18]. We intend to include the explicit pion exchange in the future development of the nonrelativistic QMC model used in the present study.

The quality of the fit is summarized in the top part of Table I and compared with the outcome of a fit with the SV-min Skyrme EDF [15] performed using the same data set and analysis. We find it encouraging that the QMC EDF, with only four adjustable parameters, yielded a rms deviation of 0.36% for binding energies, comparable with 0.24% for the Skyrme SV-min EDF. The more significant differences are in the surface thickness, diffraction radii, and the neutron pairing gaps. All these properties are sensitive to details of the region around the Fermi surface where subtle differences may occur and will be further investigated.

Using the best fit parameter set we calculated ground state binding energies of many nuclei not included in the fit. In the bottom part of Table I rms deviations between theory and experiment for 15 superheavy nuclei (SHE), 20 $N = Z$ nuclei, 22 pairs of mirror nuclei, and 170 spherical and deformed nuclei with known binding energy from isotopic chains with $Z = 38, 40, 60, 64, 86, 88, 90, 92$, and 94 and isotonic chains with $N = 20, 28, 50, 82$, and 126 are given. The most remarkable result was achieved for the SHE,

TABLE I.   Results of the fit yielding the parameters of the QMC EDF (top part). Experimental data selected by Klüpfel et al. [15] were used. Equivalent results for the Skyrme SV-min force [15] are added for comparison. rms deviations of calculated ground state binding energies from experiment for four groups of nuclei, not used in the fit of parameters, are given at the bottom part of the table. They include SHE, $N = Z$ nuclei, and $N = Z \pm 2$, 4 mirror nuclei, and chains of isotopes and isotones with $|N - Z|$ from 2 to 60, labeled "other." No experimental errors were used in calculation of rms. See text for more explanation.

| | | rms deviations | | |
| | [%] | | [absolute] | |
Data	QMC	SV-min	QMC	SV-min
Fit nuclei:				
Binding energies	0.36	0.24	2.85 MeV	0.62 MeV
Diffraction radii	1.62	0.91	0.064 fm	0.029 fm
Surface thickness	10.9	2.9	0.080 fm	0.022 fm
rms radii	0.71	0.52	0.025 fm	0.014 fm
Pairing gap (n)	57.6	17.6	0.49 MeV	0.14 MeV
Pairing gap (p)	25.3	15.5	0.052 MeV	0.11 MeV
Spin-orbit splitting (p)	15.8	18.5	0.16 MeV	0.18 MeV
Spin-orbit splitting (n)	20.3	16.3	0.30 MeV	0.20 MeV
Nuclei not included in the fit:				
Superheavy nuclei	0.10	0.32	1.97 MeV	6.17 MeV
$N = Z$ nuclei	2.54	1.44	5.89 MeV	3.47 MeV
Mirror nuclei	3.16	2.83	5.27 MeV	3.37 MeV
Other	0.51	0.30	4.27 MeV	3.19 MeV

where the absolute rms = 1.97 MeV for QMC and 6.17 MeV for SV-min (see top panel of Fig. 1). The underbinding for SV-min is a general problem in SHE for any of the standard Skyrme parametrizations [21]. The other three groups of selected nuclei reveal that the QMC rms deviation is larger then the corresponding SV-min value by a factor less than 2. This result is encouraging considering that the QMC EDF has four parameters and SV-min thirteen.

Next, we examined predictions of the QMC EDF of quadrupole (β_2), hexadecapole (β_4), and octupole (β_3) deformation parameters. Since these parameters are not observables but are extracted from experimental data in a model dependent way, we also compare QMC and SV-min results with the finite-range-droplet model (FRDM) of Moller et al. [20], which is regarded as the state-of-the-art benchmark for calculating nuclear masses and shapes. Where available, we use the quadrupole moment and lifetime of the $I^\pi = 2_1^+$ state or a lifetime-related reduced transition probability $B(E2, 0_1^+ \rightarrow 2_1^+)$. Indirect evidence for stable quadrupole deformation comes also as systematics of excited states (bands) built on the 0^+ ground states.

In Fig. 1 (bottom panel) β_2 for SHE, as calculated in QMC, SV-min, and FDRM models, are displayed. The only experimental evidence for deformation of the SHE comes

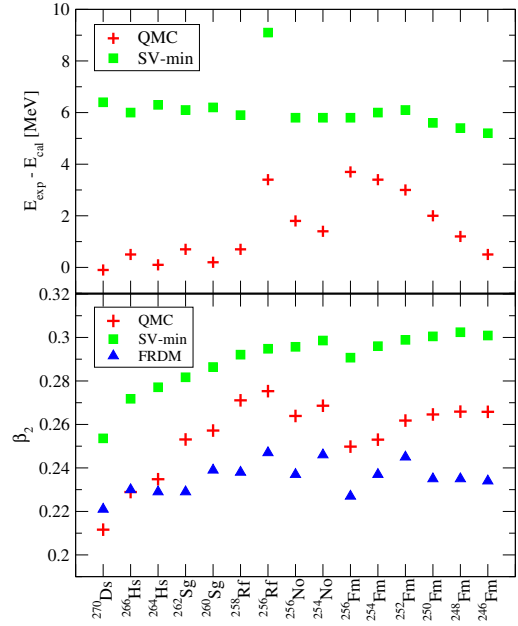

FIG. 1.   Difference between calculated and experimental ground state binding energies of SHE as obtained with QMC and SV-min EDFs (top panel). β_2 are shown in the bottom panel, which also includes FRDM [20] predictions.

from the energies of the $I^\pi = 2_1^+$ state in $^{248-256}$Fm, ^{254}No, and ^{256}Rf, which all lie in the range 44–48 keV [22,23], and the ratio $R = E(4_1^+)/E(2_1^+)$ of energies of the $I^\pi = 2_1^+$ and $I^\pi = 4_1^+$ excited states. R is between 3.24–3.52, consistent with a stable axial rotor. The ground state bands in ^{248,252,256}Fm, ^{254}No, and ^{256}Rf show a close similarity with bands observed in the neighboring U-Pu-Cm-Cf region associated with $\beta_2 = 0.27$–0.30 [24], in excellent agreement with β_2 values in Fig. 1. Thus, both the ground state binding energies and the shapes of SHE predicted by QMC are in line with other models and the scant experimental evidence.

β_2 and β_4 calculated as a function of neutron number for the Gd ($Z = 64$) isotopes are presented in Fig. 2, again in comparison with SV-min and FRDM. The predictions of QMC are almost identical with the outcome of the other models. The onset and departure from collectivity is in line with the ratio R, displayed in the bottom panel. The magnitude of β_2 extracted from $B(E2, 0_1^+ \rightarrow 2_1^+)$ is known in $^{152-160}$Gd [24] and the negative sign of the spectroscopic quadrupole moment Q_s of the $I^\pi = 2_1^+$ state [25] confirms the prolate shape of $^{152-160}$Gd. There is no experimental information on the value of β_4 but the calculation agrees well with FRDM results.

Figure 3 demonstrates that the QMC EDF reproduces the coexistence between spherical, oblate, and prolate deformation in line with many other models of $A \sim 100$ nuclei [26–31] without additional terms or change of parameters and predicts a transition from single-particle-like structure below $N = 60$ to collective behavior for higher N. Very
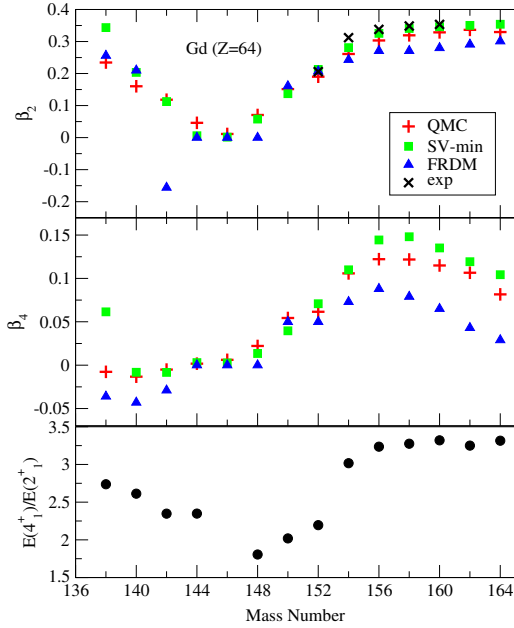
FIG. 2. Deformation parameters β_2 and β_4 of $^{138-164}$Gd ground states (top and middle panels), obtained from QMC, SV-min, and FRDM models. Experimental data [24] are added where available. Errors on β_2 and β_4 due to uncertainties in QMC EDF parameters are less than the size of the symbol used. The ratio $R = E(4_1^+)/E(2_1^+)$ is displayed in the bottom panel.

recent results results, from a Coulomb excitation experiment [32], show that deformation driving role in the $N = 60$ region remains active for Z as low as 37 and that the $A \sim 100$ region is still of active interest. We emphasise that the QMC EDF provides naturally the qualitative change in structure at $N = 60$ reported in [32].
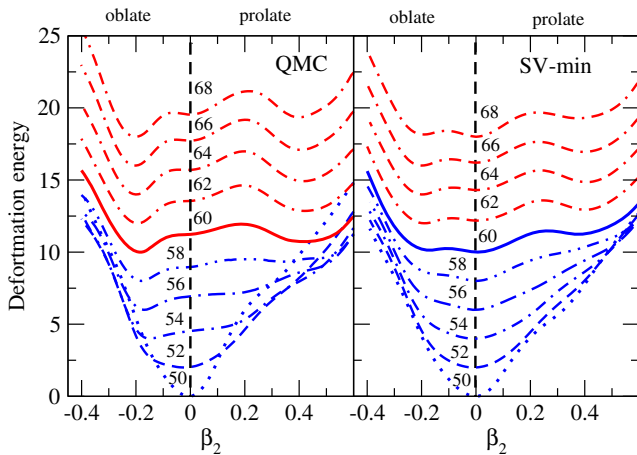

FIG. 3. Shape evolution of $^{90-106}$Zr ($Z = 40$) isotopes as a function of neutron number obtained in constrained HF + BCS with QMC (left panel) and SV-min (right panel) EDF. Deformation energies are displayed as a function of β_2. An arbitrary constant is added for each isotope, the same in both panels, for display purposes. The vertical dashed line indicates the spherical shape.

An interesting suggestion, made by Dudek *et al.* [33], that a shape of a higher order tetrahedral symmetry may occur in the ^{96}Zr ground state and compete with the quadrupole-octupole deformation, provokes the following question: is it enough to consider the traditional prolate-oblate shapes or should one seek higher order symmetries? The HF + BCS code used here does not have the capability to calculate them at this time. However, the suggestion of tetrahedral symmetry offers an incentive to improve the code and pursue this feature with the QMC interaction.

Finally, Fig. 4 demonstrates the versatility of the QMC EDF in application to quadrupole and octupole deformation in Ra and Th nuclei, again without any parameter adjustment. The evolution of β_2, β_3 with increasing neutron number is illustrated in the top (middle) for QMC (SV-min) EDF showing very similar trends, which also agree with that obtained for Th isotopes in [34]. The values of β_2 agree with experiment [24] (where available). The scarce data on β_3 provide only the magnitude but not its sign [34,35]. However, the results in Fig. 4 are supported by experimental neutron number dependence of the lowest lying $I^\pi = 2_1^+$ and $I^\pi = 1_1^-$ and $I^\pi = 3_1^-$ states in Ra and Th nuclei (bottom panel), showing close proximity of these
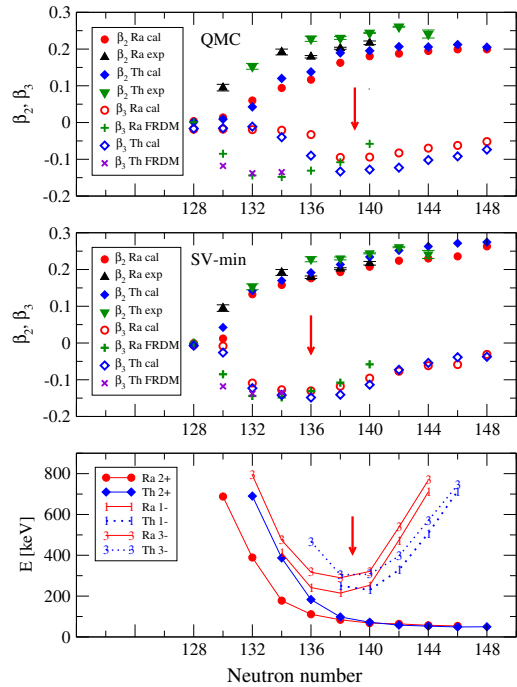

FIG. 4. Evolution of β_2 and β_3 in Ra ($Z = 88$) and Th ($Z = 90$) in the range of neutron numbers $128 \leq N \leq 148$ as predicted by the QMC (SV-min) top (middle) panel in constrained HF + BCS. Experimental data for β_2 are taken from [24]. FRDM values are added for comparison with β_3 where experimental data are not available. The arrows indicate the maximum octupole deformation. Experimental 2_1^+, 1_1^-, and 3_1^- excitation energies [22], are displayed in the bottom panel where lines are added to guide the eye. For more explanation see text.

states to the ground state for $138 \leq N \leq 140$. The QMC model is in agreement with this data in that the maximum $|\beta_3|$ and the saturation of β_2 is found at $138 \leq N \leq 140$. SV-min and FRDM result are marginally different in predicting $|\beta_3|$ to reach a maximum at $N = 136$ [see the (red) arrows in Fig. 4].

In summary, we have demonstrated for the first time that the QMC EDF, in its present form, predicts properties of even-even nuclei across the nuclear chart on a level comparable with the Skyrme EDF which has many more parameters. The novelty of this approach is that we have introduced fundamentally new physics into the EDF. Modeling the nuclear medium effect through the modification of the internal structure of the nucleon is unique to the QMC approach and has not been previously applied to nuclei to the extent reported here. That in turn led to a novel, microscopically derived density dependence. The calibrated parameters are a single, universally applicable set of four, in contrast to the larger parameter sets used in the Skyrme-Hartree-Fock mean-field models, often locally fine tuned and lacking universality. The QMC model is still at an early stage of development and the aim of this Letter has been to examine its promise as compared to other models. Among the many levels of sophistication to consider is the inclusion of an explicit pion exchange component, known to reduce the incompressibility of nuclear matter. It will be especially interesting to explore QMC predictions for nuclei near the limits of stability and, given its demonstrated accuracy for SHE, for potential islands of stability at very large mass number.

[1] D. Vautherin and D. M. Brink, Phys. Rev. C **5**, 626 (1972).
[2] M. Bender, P.-H. Heenen, and P.-G. Reinhard, Rev. Mod. Phys. **75**, 121 (2003).
[3] J. R. Stone and P.-G. Reinhard, Prog. Part. Nucl. Phys. **58**, 587 (2007).
[4] P.-G. Reinhard, Phys. Scr. **91**, 023002 (2016).
[5] P. A. M. Guichon, Phys. Lett. B **200**, 235 (1988).
[6] P. A. M. Guichon, K. Saito, E. N. Rodionov, and A. W. Thomas, Nucl. Phys. **A601**, 349 (1996).
[7] T. A. DeGrand, R. L. Jaffe, K. Johnson, and J. E. Kiskis, Phys. Rev. D **12**, 2060 (1975).
[8] P. A. M. Guichon, H. H. Matevosyan, N. Sandulescu, and A. W. Thomas, Nucl. Phys. **A772**, 1 (2006).
[9] E. Chabanat, P. Bonche, P. Haensel, J. Meyer, and R. Schaeffer, Nucl. Phys. **A627**, 710 (1997).
[10] A. W. Thomas, P. A. M. Guichon, D. B. Leinweber, and R. D. Young, Prog. Theor. Phys. Suppl. **156**, 124 (2004).
[11] P. A. M. Guichon and A. W. Thomas, Phys. Rev. Lett. **93**, 132502 (2004).
[12] K. Tsushima, K. Saito, and A. W. Thomas, Phys. Lett. B **411**, 9 (1997); **421**, 413(E) (1998).
[13] P. A. M. Guichon, A. W. Thomas, and K. Tsushima, Nucl. Phys. **A814**, 66 (2008).
[14] P. G. Reinhard (private communication).
[15] P. Klüpfel, P.-G. Reinhard, T. J. Bürvenich, and J. A. Maruhn, Phys. Rev. C **79**, 034310 (2009).
[16] D. L. Whittenbury, J. D. Carroll, A. W. Thomas, K. Tsushima, and J. R. Stone, Phys. Rev. C **89**, 065801 (2014).
[17] J. P. Blaizot, Phys. Rep. **64**, 171 (1980).
[18] J. R. Stone, N. J. Stone, and S. A. Moszkowski, Phys. Rev. C **89**, 044316 (2014).
[19] J. R. Stone, P. A. M. Guichon, H. H. Matevosyan, and A. W. Thomas, Nucl. Phys. **A792**, 341 (2007).
[20] P. Moller, J. R. Nix, W. D. Myers, and W. J. Swiatecki, At. Data Nucl. Data Tables **59**, 185 (1995).
[21] P.-G. Reinhard, M. Bender, and J. A. Maruhn, Comm. Mod. Phys. A **2**, 177 (2002).
[22] National Nuclear Center (NNDC), http://www.nndc.bnl.gov/.
[23] P. T. Greenless et al., Phys. Rev. Lett. **109**, 012501 (2012).
[24] S. Raman, C. W. Nestor, Jr., and P. Tikkanen, At. Data Nucl. Data Tables **78**, 1 (2001).
[25] N. J. Stone, At. Data Nucl. Data Tables **90**, 75 (2005).
[26] P.-G. Reinhard, D. J. Dean, W. Nazarewicz, J. Dobaczewski, J. A. Maruhn, and M. R. Strayer, Phys. Rev. C **60**, 014316 (1999).
[27] M. Kortelainen, T. Lesinski, J. More, W. Nazarewicz, J. Sarich, N. Schunck, M. V. Stoitsov, and S. Wild, Phys. Rev. C **82**, 024313 (2010).
[28] R. Rodriguez-Guzman, P. Sarriguren, L. M. Robledo, and S. Perez-Martin, Phys. Lett. B **691**, 202 (2010).
[29] Y.-X. Liu, Y. Sun, X.-H. Zhou, Y.-H. Zhang, S.-Y. Yu, Y.-C. Yang, and H. Jin, Nucl. Phys. **A858**, 11 (2011).
[30] J. Xiang, Z. P. Li, Z. X. Li, J. M. Yaoa, and J. Meng, Nucl. Phys. **A873**, 1 (2012).
[31] H. Mei, J. Xiang, J. M. Yao, Z. P. Li, and J. Meng, Phys. Rev. C **85**, 034321 (2012).
[32] C. Sotty et al., Phys. Rev. Lett. **115**, 172501 (2015).
[33] J. Dudek, D. Curien, D. Rouvel, K. Mazurek, Y. R. Shimizu, and S. Tagami, Phys. Scr. **89**, 054007 (2014).
[34] Z. P. Li, B. Y. Song, J. M. Yao, D. Vretenar, and J. Meng, Phys. Lett. B **726**, 866 (2013).
[35] L. P. Gaffney et al., Nature (London) **497**, 199 (2013).